

## 1. Introduction

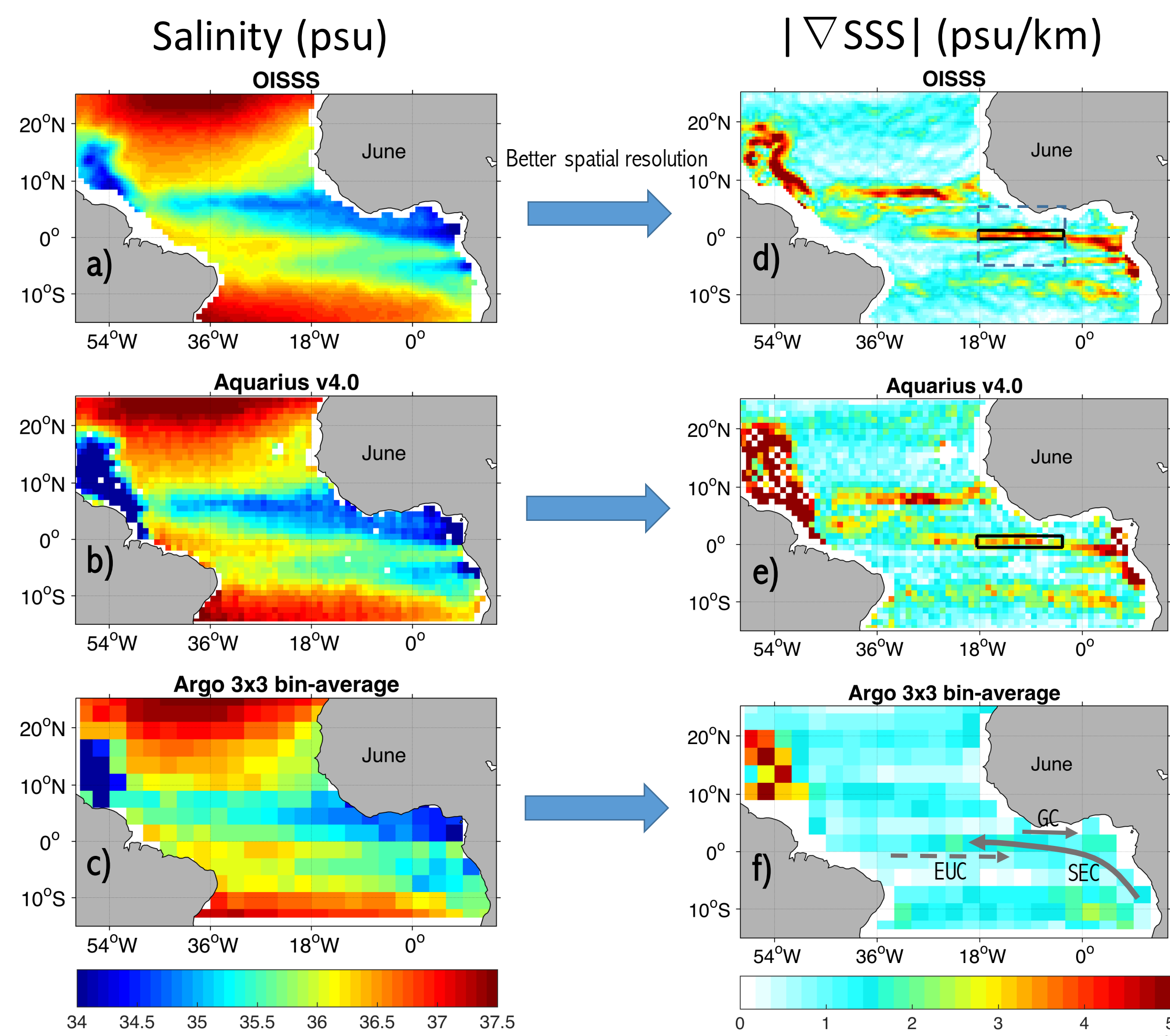


Fig. 1: SSS in the tropical Atlantic (left column) for a) Aquarius OI (Melnichenko et al., 2016), b) Aquarius v 4.0, c) Argo 3x3 bin-average and (d-f) the corresponding gradient fields ( $|\nabla SSS|$ , psu/km) (right column). The mean currents are indicated with gray arrows. GC: Guinea current, EUC: Equatorial undercurrent, SEC: South equatorial current. The black boxes in the Fig. 1d) and 1e) indicate the area selected to compute the spatial average in Fig. 6.

The Equatorial Atlantic Ocean is a region dominated by the seasonal trade winds and Intertropical Convergence Zone (ITCZ). It is also marked by the existence of a strong sea surface temperature (SST) front due to the formation of the equatorial cold tongue. It is believed that these features have strong effects on the atmospheric circulation in the region and thus climate.

The release of high-resolution salinity products allow us to study salinity fronts. We use three years of sea surface salinity (SSS) observations from Aquarius satellite to investigate the spatial structure, temporal variability, and driving dynamics of the frontal SSS feature in the equatorial Atlantic.

## 2.1 Results: Spatial and temporal variability of the front

$$SSS \text{ front} = |\nabla SSS| > 0.002 \text{ psu/km}$$

- SSS front starts in April and amplifies in May-June (Fig. 2a).
- The front extends from the coast of Africa to  $\sim 29^\circ\text{W}$  (Fig. 1d). It separates fresh water (blue arrow) in the north and salty water (red arrow) in the south of the Equator (Fig. 2b).
- SSS and SST gradients maximize at the same latitude, between  $0^\circ$  and  $1^\circ\text{N}$  (Fig. 2a and c).
- SST front peaks in June-July, one month after the SSS front (Fig. 2a and c, Fig. 6a).
- Density gradient peaks in June due to the contribution of SST and SSS gradients.

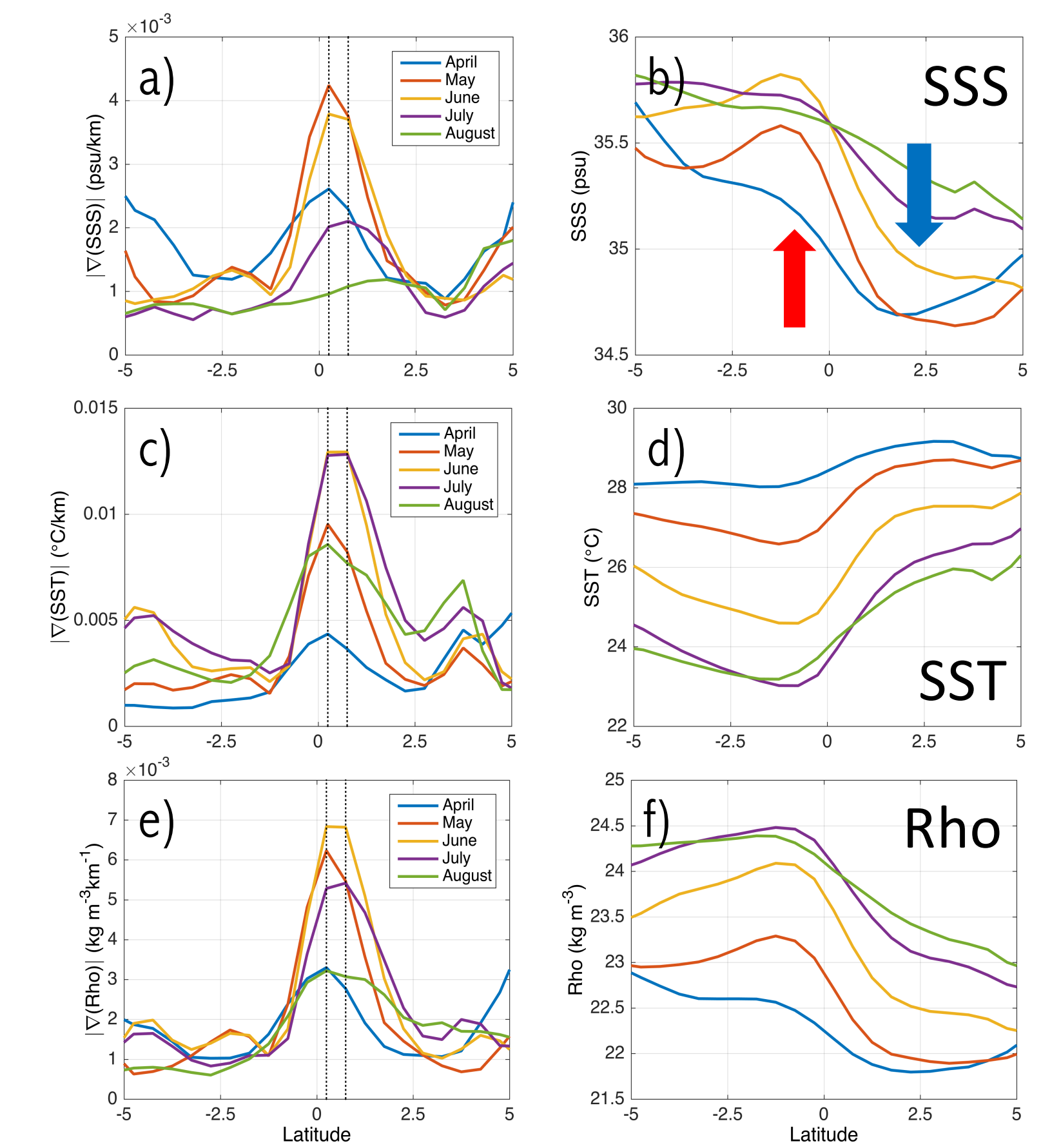


Fig. 2: Meridional profiles of gradient (left column) and values (right column) of SSS (a, b), Reynolds SST (c, d) and density (e, f) for climatological months when the equatorial front is present. The longitudinal average is between  $18^\circ\text{W}$  and  $4^\circ\text{W}$  (gray box Fig. 1d).

## 2.3 Results: Interannual variability of the SSS gradient

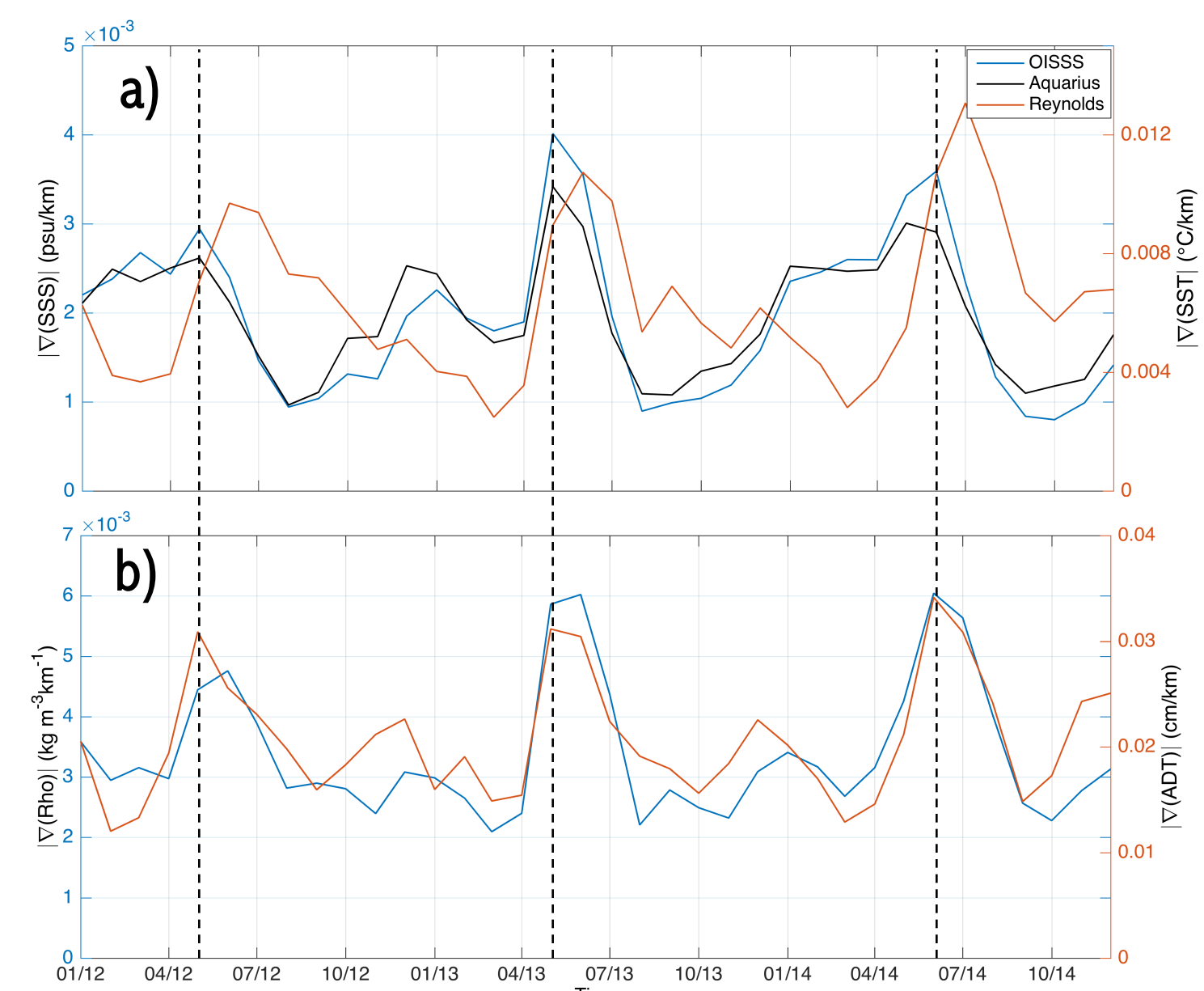


Fig. 6: Monthly time series of magnitude of the gradient of a) salinity (OISSS blue line, Aquarius v4.0 black line), temperature (red line), b) absolute dynamic topography (red line) and density (blue line). The spatial average is indicated in Fig. 1d and e with the black box.

- SSS gradient peaks in May, except in 2014.
- The strongest magnitude is in May 2013, and the weakest in 2012.
- SST gradient is stronger in July 2014 than June 2013 and 2012.
- SSS front does not last as long as the SST front.
- Density gradient is mainly dominated by SST and effects of SSS changes are secondary.
- The maximum SSS gradient affects the density, observing the density gradient peaked in June 2014.
- There is a good coherence between density gradient and Absolute dynamic topography (ADT, AVISO) gradient.

- What can cause the interannual variability in the salinity front? The causes might be related with wind stress, freshwater flux and horizontal advection. The Hovmöller of the wind stress (Fig. 7) indicates that the wind increases year after year in agreement with the SST gradient.

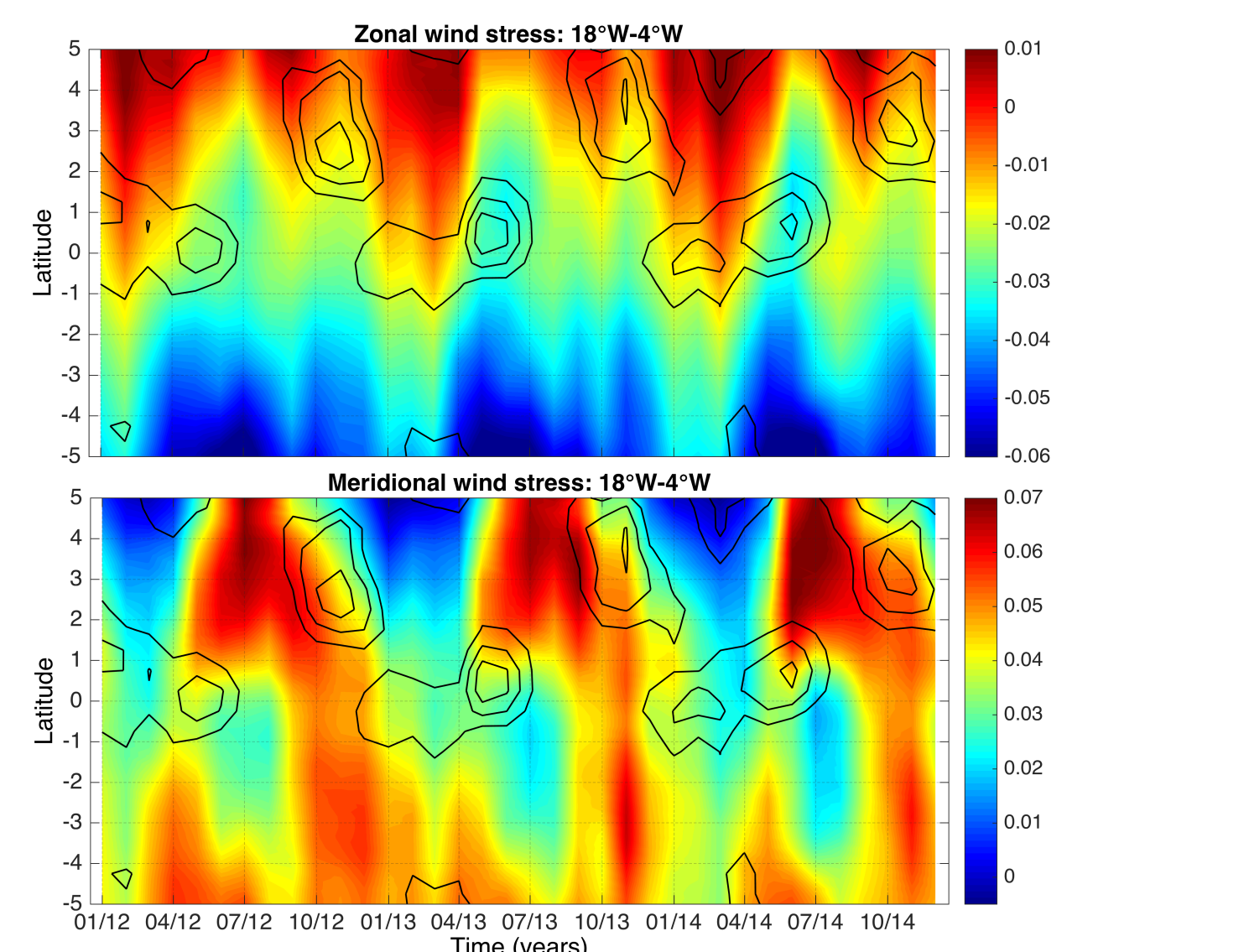


Fig. 7: Latitude-time plots of the monthly zonal (upper) and meridional (bottom) wind stress (units: Pa, ASCAT) average between  $18^\circ\text{W}$  and  $4^\circ\text{W}$  (gray dashed box Fig. 1d). Black contours correspond to the  $|\nabla SSS|$  equal to 0.002, 0.003 and 0.004 psu/km.

- E-P also presents an interannual variability finding that the negative values (more fresh water) reached a southern latitude in 2013 (Fig. 8a). This is in agreement with the SSS Hovmöller (Fig. 8b).

## 3. Conclusions

- Aquarius OISSS allows to characterize the salinity fronts in the Tropical Atlantic with a better detail.
- It is possible to describe the vertical structure of the front collecting Argo profiles within a longitude range of more than 15 degrees and at climatological scale.
- The salinity front at the Equator is evident in boreal summer (May-June) and is triggered by the EUC.
- The front weakens rapidly due to an increment in the SSS north of the Equator, partly explained by the freshwater flux.
- The interannual variability of the front is not well understood yet. Preliminary results indicate that the strongest SSS gradient in 2013 might be related with E-P.

## 2.2 Results: Vertical structure of the front

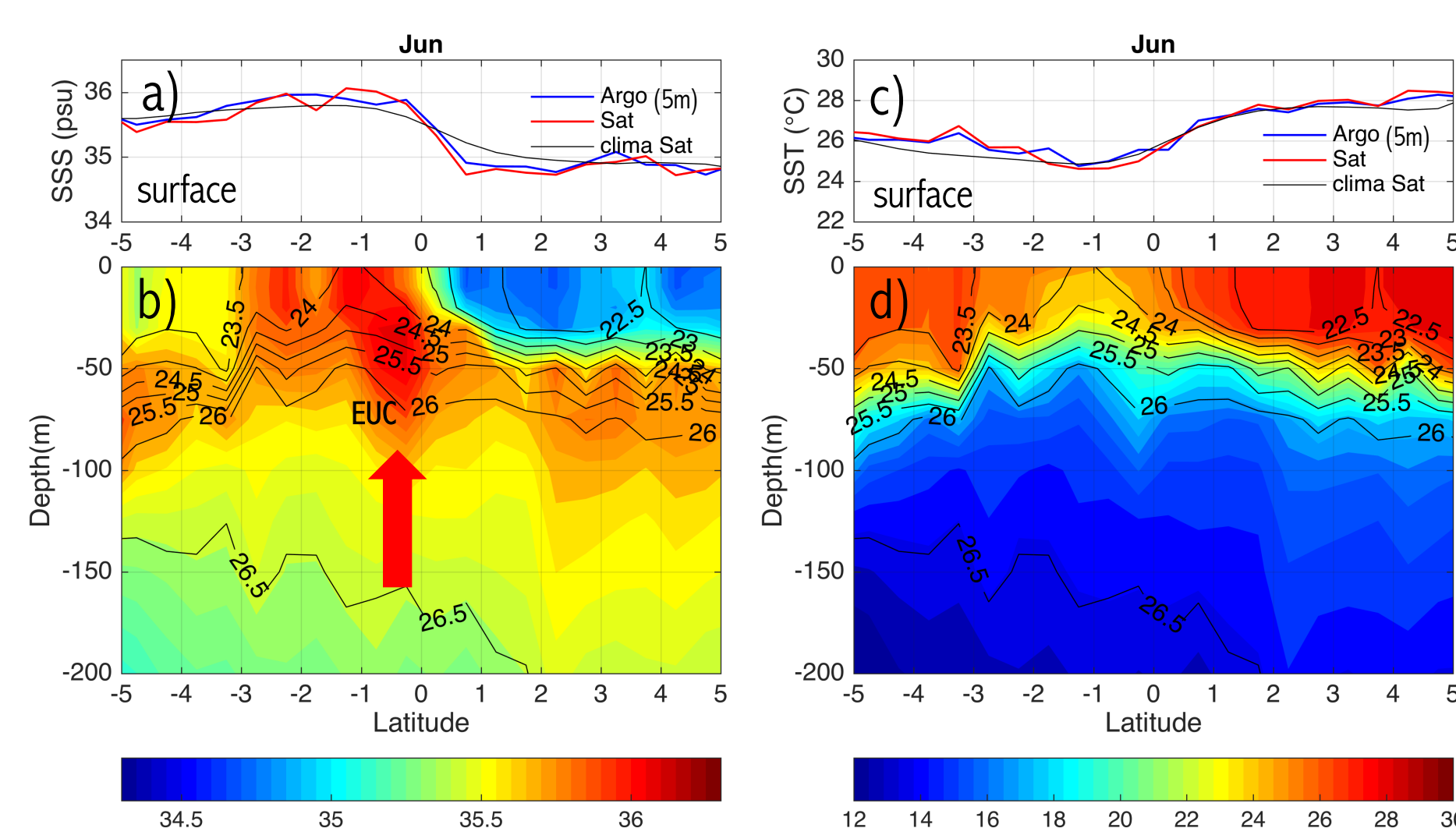


Fig. 4: Meridional vertical section of salinity (a, b) and temperature (c, d) referred to the position of salinity front derived from Argo profiles. The sections include all the profiles between  $20^\circ$  and  $0^\circ\text{W}$  during June and October 2012, 2013 and 2014. In situ measurements were binned on a  $0.5^\circ$  grid.

- The salty anomaly observed in the isopycnal layer  $24.5\text{-}26.2 \text{ kg/m}^3$  (south of Equator, fig 4-5) related with the EUC is in agreement with Johns et al. (2014) and others.
- The salinity of EUC peaks twice per year (Johns et al., 2014; Da Allada et al., 2017). Fig. 5 represents those peaks and it also indicates that the condition to generate the salinity front is only given in May. During October, the meridional salinity gradient is weak, since the fresh pool is located north of  $3^\circ\text{N}$ .

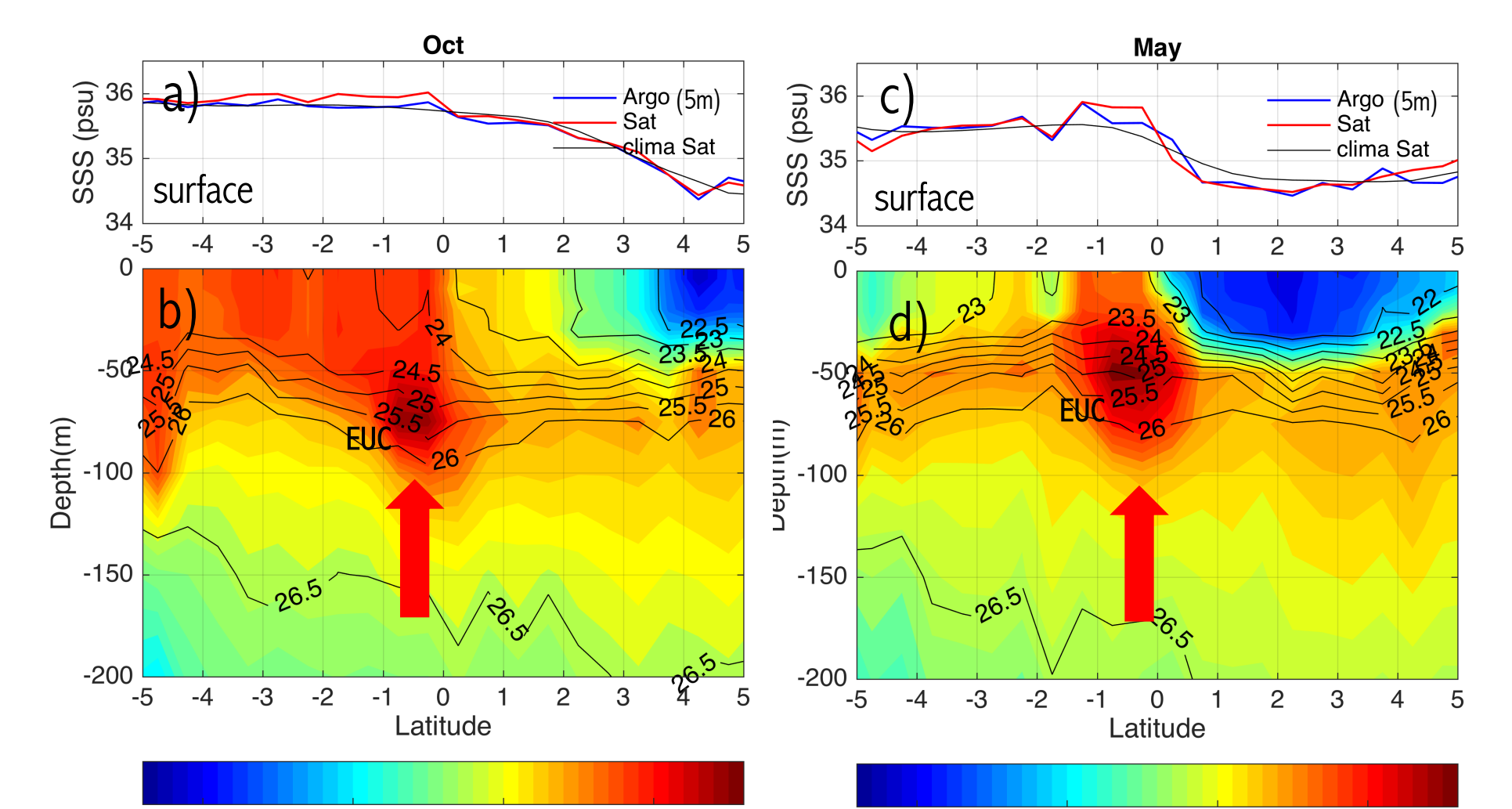


Fig. 5: Meridional vertical section of salinity (a, b) and temperature (c, d) referred to the position of salinity front derived from Argo profiles. The sections include all the profiles between  $20^\circ$  and  $0^\circ\text{W}$  during October and May 2012, 2013 and 2014. In situ measurements were binned on a  $0.5^\circ$  grid.

- The increment in salinity south of the equator triggers the SSS front (Fig. 2b, Fig. 3b). This is related with the subsurface EUC when vertical mixing translates the signature of its salty core to the surface (Da Allada et al., 2017).
- The front weakens because salinity increases north of the Equator at a larger rate than the EUC signal decreases (Fig. 3c-d).
- Part of the increment in salinity is due to the positive freshwater flux (Fig. 3g-h).

- Figs. 4a-b and Fig. 5a-c show the good agreement between OISSS and Argo data at 5m.

## References

Melnichenko, O., Hacker, P., Maximenko, N., Lagerloef, G., & Potemra, J. (2016). Optimum interpolation analysis of Aquarius sea surface salinity. *Journal of Geophysical Research: Oceans*, 121(1), 602-616; Reynolds, R.W., N.A. Rayner, T.M. Smith, D.C. Stokes, and W. Wang, 2002: An improved in situ and satellite SST analysis for climate. *J. Climate*, 15, 1609-1625, doi:10.1002/2015JC010790; NASA Aquarius project. 2015. Aquarius Official Release Level 3 Sea Surface Salinity Standard Mapped Image 7-Day Data V4.0. Ver. 4.0. PO.DAAC, CA, USA. Dataset accessed [YYYY-MM-DD] at <http://dx.doi.org/10.5067/AQR40-357CS>; Da-Allada, C. Y., Jouanno, J., Gaillard, F., Kolodziejczyk, N., Maes, C., Reul, N., & Bourlès, B. (2017). Importance of the Equatorial Undercurrent on the sea surface salinity in the eastern equatorial Atlantic in boreal spring. *Journal of Geophysical Research: Oceans*, 122(1), 521-538; Johns, W. E., Brandt, P., Bourlès, B., Tanet, A., Papapostolou, A., & Houk, A. (2014). Zonal structure and seasonal variability of the Atlantic Equatorial Undercurrent. *Climate dynamics*, 43(11), 3047-3069.

## Acknowledge

This study is supported through NASA Ocean Salinity Science Team grants NNX14AJ64G, NNX17AK12G and NNX14AJ02G. The gridded Argo product is produced by the Asia-Pacific Data Research Center (APDRC) of the University of Hawaii; available at <http://apdrc.soest.hawaii.edu/projects/argo/>. NOAA\_OI\_SST\_V2 data provided by the NOAA/OAR/ESRL PSD, Boulder, Colorado, USA, from their Web site at <http://www.esrl.noaa.gov/psd/>.